



## Label-free electrochemical detection of singlet oxygen protein damage



Veronika Vargová<sup>a</sup>, Rodrigo E. Giménez<sup>b</sup>, Hana Černocká<sup>a</sup>, Diana Chito Trujillo<sup>b</sup>,  
Fiorella Tulli<sup>b</sup>, Verónica I. Paz Zanini<sup>b</sup>, Emil Paleček<sup>a</sup>, Claudio D. Borsarelli<sup>b</sup>,  
Veronika Ostatná<sup>a,\*</sup>

<sup>a</sup> Institute of Biophysics, Academy of Sciences of the Czech Republic, v.v.i., Královopolská 135, 612 65 Brno, Czech Republic

<sup>b</sup> Instituto de Bionanotecnología, INBIONATEC-CONICET, Universidad Nacional de Santiago del Estero (UNSE), RN 9, Km 1125, G4206XCP Santiago del Estero, Argentina

### ARTICLE INFO

#### Article history:

Received 17 September 2015

Received in revised form 19 November 2015

Accepted 19 November 2015

Available online 22 November 2015

#### Keywords:

singlet oxygen protein damage  
surface-attached protein stability  
mercury and carbon electrodes  
constant current chronopotentiometry  
square wave voltammetry

### ABSTRACT

Oxidative damage of proteins results in changes of their structures and functions. In this work, the singlet oxygen (<sup>1</sup>O<sub>2</sub>)-mediated oxidation of bovine serum albumin (BSA) and urease by blue-light photosensitization of the tris(2,2'-bipyridine)ruthenium(II) cation [Ru(bpy)<sub>3</sub>]<sup>2+</sup> was studied by square wave voltammetry at glassy carbon electrode and by constant current chronopotentiometry at mercury electrode. Small changes in voltammetric oxidation Tyr and Trp peaks did not indicate significant changes in the BSA structure after photo-oxidation at carbon electrode. On the other hand chronopotentiometric peak H of BSA at HMDE increased during blue-light photosensitization, indicating that photo-oxidized BSA was more susceptible to the electric field-induced denaturation than non-oxidized native BSA. Similar results were obtained for urease, where enzymatic activity was also evaluated. The present results show the capability of label- and reagent-free electrochemical methods to detect oxidative changes in proteins. We believe that these methods will become important tools for detection of various protein damages.

© 2015 Elsevier Ltd. All rights reserved.

## 1. Introduction

Proteins are one of the major targets for oxidative damage in the cell. Indirect non-radical oxidation of the protein via formation and subsequent reaction with singlet oxygen (<sup>1</sup>O<sub>2</sub>) is one of the major processes. <sup>1</sup>O<sub>2</sub>-mediated oxidation induces several biophysical and biochemical changes in proteins, such as an increase in susceptibility of the oxidized protein to proteolytic enzymes, alterations in mechanical properties, an increased extent or predisposition to unfolding, changes in conformation, an increase in hydrophobicity and changes in binding of co-factors and metal ions (reviewed in [1–3]). The extent of component damage does not need to correlate with the importance of damage. Thus a low level of damage to critical species may be of much greater significance than massive damage to a nonessential target. Oxidative damage in proteins has been studied by high-performance liquid chromatography, fluorescence spectroscopy, mass spectroscopy, 2D electrophoresis, electron paramagnetic

resonance, Raman resonance [2–4], while the use of electrochemical methods for this purpose is still infrequent [5–7]. Wang et al. studied BSA damage by Fenton reaction mediated by the hydroxyl radical \*OH, where the differential pulse voltammetric oxidation signal of electroactive indicator (2,2'-bipyridyl) cobalt(III) perchlorate decreased in correlation with BSA damage [7]. Indeed, \*OH is one of the most reactive oxygen species that markedly non-selectively reacts with proteins, inducing protein damage such as protein fragmentation [3].

Electrochemistry of proteins boomed in the last decades, but it has focused on electroactivity of non-protein redox centers (such as metal ions) in relatively small number of conjugated proteins, being thus of little use in proteomics studying thousands of proteins [8,9]. A couple of studies of non-conjugated proteins were done using voltammetry at graphite electrodes [10–13] and impedance spectroscopy at metal electrodes [14]. We showed that chronopotentiometric stripping in combination with mercury-containing electrodes is suitable tool for label-free protein detection [13] including proteins important in biomedicine [12,15–18]. Nano and subnano-molar concentrations of proteins can be detected at lower stripping current intensities [13,19], while conformational changes in proteins [13,20,21] and also protein-DNA [22] interactions can be studied at higher current intensities.

\* Corresponding author at: Institute of Biophysics ASCR, v.v.i., Královopolská 135, 612 65 Brno, Czech Republic. Tel.: +420 541 517 162; fax: +420 541 517 249.  
E-mail address: [ostatna@ibp.cz](mailto:ostatna@ibp.cz) (V. Ostatná).

In this paper, we present new label- and reagent-free electrochemical methods suitable for detection of oxidative changes in proteins. We chose the non-radical oxidant  $^1\text{O}_2$ , which selectively reacts with electron-rich amino acid (aa) residues in proteins, such as Met, Cys, His, Tyr and Trp [3].  $^1\text{O}_2$  is more efficiently produced in tissues by UVA or visible light photosensitized reactions involving several endogenous and exogenous sensitizer molecules [23,24]. In our study, we followed BSA oxidative changes produced after blue-light photosensitization of tris(2,2'-bipyridine) ruthenium(II) cation ( $\text{Ru}(\text{bpy})_3^{2+}$ ) that generates  $^1\text{O}_2$ , by square wave voltammetry (SWV) at glassy carbon electrode (GCE) and by constant current chronopotentiometry (CPS) at mercury electrode. At carbon electrode no large  $^1\text{O}_2$ -mediated changes in the BSA voltammetric responses were detected. On the other hand CPS analysis at mercury electrode indicated that photo-oxidized surface-attached BSA and urease were destabilized and more susceptible to the electric field-induced denaturation.

## 2. Experimental

### 2.1. Materials

Bovine serum albumin, urease from jack bean, amino acids, polyamino acids and reagents of the highest available quality were received from Sigma-Aldrich. Solutions were prepared in triply-distilled water.

### 2.2. Electrochemical measurements

Voltammetric measurements were performed with  $\mu\text{Autolab III}$  analyzer (Eco Chemie, Utrecht, The Netherlands) in connection with VA-Stand 663 (Metrohm, Herisau, Switzerland). Three-electrode system were used containing  $\text{Ag}|\text{AgCl}|3\text{M KCl}$  electrode as a reference and platinum wire as an auxiliary electrode. A hanging mercury drop electrode (HMDE,  $0.4\text{ mm}^2$ , Metrohm, Switzerland) or a glassy carbon electrode (GCE, area  $3.14\text{ mm}^2$ ) were used as working electrodes. The cleaning procedure of the GCE included polishing with alumina  $0.3\text{ }\mu\text{m}$  on soft lapping pads for 2 min followed by sonication by Fisherbrand FB 11020 in deionized water for 2 min. All measurements were performed at  $26^\circ\text{C}$  open to air. CPS measurements at HMDE: stripping current,  $I_{\text{str}} -35\text{ }\mu\text{A}$  (if not stated otherwise). Square wave voltammetry (SWV) at GCE: amplitude  $10\text{ mV}$ ; step  $10\text{ mV}$ , frequency  $25\text{ Hz}$ . Voltammograms were baseline corrected with moving average employing the built-in GPES software.

### 2.2.1. Adsorptive (Ad, in situ) stripping at HMDE

BSA or aa's were adsorbed at accumulation potential,  $E_A + 0.1\text{ V}$  for accumulation time,  $t_A$  60 s from  $50\text{ mM}$  Na-phosphate pH 7 followed by chronopotentiogram recording. Stirring accompanied accumulation.

### 2.2.2. Adsorptive stripping at GCE

BSA or aa's were adsorbed at  $E_A + 0.1\text{ V}$  for  $t_A$  300 s from  $50\text{ mM}$  Na-phosphate pH 7 followed by SW voltammogram recording. Stirring accompanied accumulation.

### 2.2.3. Adsorptive Transfer (AdT, ex situ) at HMDE[25]

Proteins were adsorbed from  $5\text{ }\mu\text{L}$  drop of  $1\text{ }\mu\text{M}$  protein sample (if not stated otherwise) in  $50\text{ mM}$  Na-phosphate pH 7 at open current potential for 2 min, followed by washing, transferring of protein modified HMDE to blank electrolyte and recording of chronopotentiogram.

### 2.2.4. Adsorptive Transfer (AdT, ex situ) at GCE

Proteins were adsorbed from  $15\text{ }\mu\text{L}$  drop of  $1\text{ }\mu\text{M}$  protein sample (if not stated otherwise) in  $50\text{ mM}$  Na-phosphate pH 7 at open current potential for 5 min, followed by washing, transferring of protein modified GCE to blank electrolyte and recording of SW voltammogram.

### 2.3. Steady-state photolysis experiments

A home-made steady-state photolysis system was built by focusing a blue LED ( $443 \pm 21\text{ nm}$ ,  $1\text{ W}$ ) as selective excitation source of  $\text{Ru}(\text{bpy})_3^{2+}$ . Photolysis of air-saturated solutions was performed with  $10\text{ }\mu\text{M}$  BSA (or  $1\text{ mM}$  aa's or  $50\text{ }\mu\text{g/mL}$  polyamino acids) in presence of  $20\text{ }\mu\text{M}$   $\text{Ru}(\text{bpy})_3^{2+}$  in  $50\text{ mM}$  Na-phosphate pH 7. Soft magnetic stirring of protein solution was done to avoid foam formation.

### 2.4. Urease activity measurements

#### 2.4.1. In solution

$0.05\text{ }\mu\text{M}$  urease was incubated in  $100\text{ }\mu\text{L}$  of  $1\text{ M}$  urea with  $0.1\%$  bromocresol purple for 5 min at  $25^\circ\text{C}$  and absorption spectra were recorded on NanoDrop 1000 spectrophotometer with optical path length  $1\text{ mm}$  [20,26].

#### 2.4.2. At surface

Solid Ag-amalgam rod (Metrohm Switzerland) was prepared by brushing and dipping into mercury for several minutes and

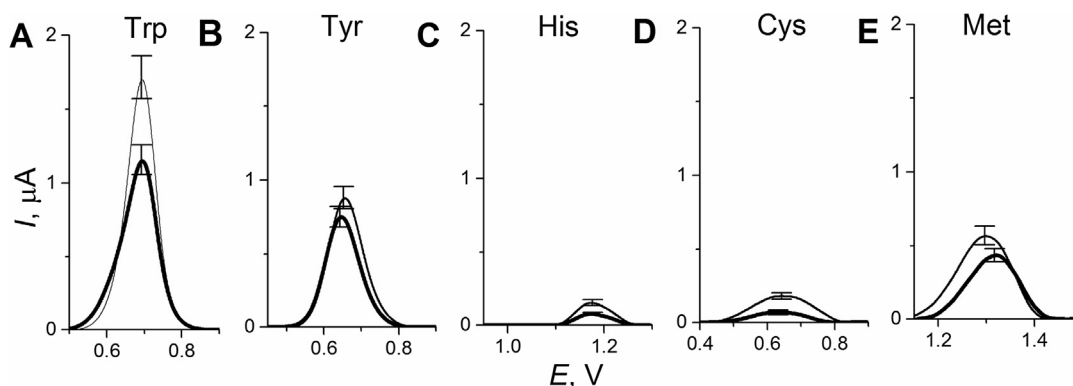


**Fig. 1.** *In situ* SW voltammograms of oxidation peaks of amino acids.  $100\text{ }\mu\text{M}$  A. Trp, B. Tyr C. His D. Cys and E.  $500\text{ }\mu\text{M}$  Met in presence of A. - D.  $2\text{ }\mu\text{M}$  E.  $10\text{ }\mu\text{M}$   $\text{Ru}(\text{bpy})_3^{2+}$  after (thick line —) or without (thin line —) 60 min photosensitization with blue light. Amino acids were adsorbed for 300 s at  $0.1\text{ V}$  at GCE and then SW voltammogram was recorded in  $50\text{ mM}$  Na-phosphate pH 7. Amino acids solutions containing  $\text{Ru}(\text{bpy})_3^{2+}$  under dark conditions yielded the same peaks as amino acids in absence of  $\text{Ru}(\text{bpy})_3^{2+}$ .

cleaned in 20% nitric acid for 10 s followed by washing in 96% ethanol. Urease was adsorbed on a bare amalgam rod by dipping the rod into 150  $\mu\text{L}$  of 50  $\mu\text{M}$  urease solution for  $t_A$  10 min (without stirring) at 25  $^\circ\text{C}$ . The rod was then washed with water and immersed in 100  $\mu\text{L}$  of 1 M urea with 0.1% bromocresol purple for 2 min and absorption spectra were recorded at 592 nm [20].

### 3. Results and discussion

#### 3.1. Detection of $^1\text{O}_2$ -induced protein damage at carbon electrodes

##### 3.1.1. Electro-oxidation of monomeric amino acids

$^1\text{O}_2$  can react with protein backbone sites or with electron-rich side chains of aa's such as His, Trp, Tyr, Met and Cys [27–29].  $^1\text{O}_2$ -mediated oxidation of Trp residues in human and bovine serum albumins have been directly monitored by fluorescence spectroscopy [30,31], but oxidation of Cys, Met or His are not detectable by direct spectroscopic measurements. The above mentioned aa's can be electro-oxidized in their monomeric states or in short peptides at carbon electrodes [13,32]. 100  $\mu\text{M}$  Trp, Tyr, Cys or His, adsorbed from 50 mM Na-phosphate pH 7, yielded oxidation peaks with different magnitudes at different peak potentials ( $E_p$ 's, Fig. 1). Trp showed the largest oxidation peak at potential  $E_p$  of +0.70 V, while the Tyr peak was about half of the Trp signal and shifted by about 50 mV to less positive potentials. Cys peak at about +0.65 V and peak of His at +1.1 V were 10-times smaller than Trp peak. We did not observe any oxidation peak of Met at its 100  $\mu\text{M}$  concentration but 500  $\mu\text{M}$  Met yielded peak at the most positive potential,  $E_p$  + 1.3 V.

Air-saturated solutions of 1 mM amino acid were irradiated with blue light for 60 min to excite selectively the photosensitizer  $\text{Ru}(\text{bpy})_3^{2+}$  (20  $\mu\text{M}$ ), which generates  $^1\text{O}_2$  with a quantum yield of about 40% [33]. After irradiation treatment, samples were diluted 10 times (or twice for Met) in electrochemical cell. Less than 10% decrease of Tyr peak was observed after photolysis (Fig. 1B), that is the value close to the experimental error. Peak of Met decreased by  $\sim 20\%$ , Trp  $\sim 40\%$ , His  $\sim 50\%$  and Cys peak even  $\sim 60\%$  after 1 hour irradiation (Fig. 1). The relative SWV peak diminution of these aa residues was proportional to their chemical reactivity towards  $^1\text{O}_2$ , Eq. (1), since under the present pH conditions, the magnitude of the chemical rate constant, i.e.  $k_c$  followed the trend Tyr < Met < Trp  $\approx$  His  $\approx$  Cys [28,29].



##### 3.1.2. Electro-oxidation of amino acids residues in proteins

Electro-oxidation of Tyr (peak Y) and Trp residues (peak W) in proteins was described at carbon electrodes [11,13,34]. In the protein voltammograms, peaks Y and W are usually overlapped (YW peak), while they can be separated in short peptides and smaller proteins [35]. Cys monomer oxidized at similar potentials as Tyr and Trp residues (Fig. 1). It could be speculated that also Cys residues may contribute to YW peak, but up to now contribution of Cys residues in proteins was not experimentally proved. His electro-oxidation was described for His-tagged proteins [12].

Selection of carbon electrode type appears important in protein structure studies [11,12]. GCE as well as the edge plane oriented pyrolytic graphite electrodes seemed to be sensitive for structural changes of proteins [11]. Using GCE, we observed peak of native BSA about 3.5-times smaller than that of urea-denatured BSA (Fig. 2A) in good agreement with previous results [11,12]. Higher YW peak in denatured BSA than in native BSA suggests larger accessibility and adsorbability of aa's residues resulting from BSA denaturation [11,13]. Changes of YW peak were observed also after BSA photo-oxidation in presence of photosensitizer (see below).

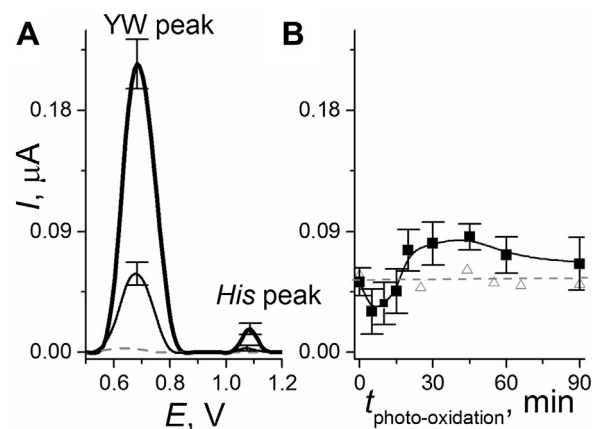


**Fig. 2.** A *In situ* SW voltammogram YW peak of 1  $\mu\text{M}$  native (—) and urea-denatured (---) BSA in background electrolyte (50 mM Na-phosphate pH 7, ---). B. Dependence of peak height of native BSA (■) on photo-oxidation time. 1  $\mu\text{M}$  BSA in presence of 2  $\mu\text{M}$   $\text{Ru}(\text{bpy})_3^{2+}$  was adsorbed at 0.1 V for accumulation time,  $t_A$  300 s from 50 mM Na-phosphate pH 7 at GCE, followed by SW voltammogram recording. Control done with native BSA at the same experimental setup under dark conditions (—Δ—).

His peak of native BSA (at +1.1 V) was too small for studies of its changes during photo-oxidation.

##### 3.1.3. Electro-oxidation of amino acid residues in photo-oxidized BSA

Photosensitized  $^1\text{O}_2$  generation with  $\text{Ru}(\text{bpy})_3^{2+}$  in air-saturated BSA solutions was performed in the bulk of aqueous buffer, since the metal complex did not form adduct with BSA [36]. Hence, protein oxidation occurred by free diffusion of  $^1\text{O}_2$  in the aqueous buffer, because this reactive oxygen species was able to travel at least an average distance about 2-order of magnitude larger than the BSA diameter during its lifetime ( $\approx 3 \mu\text{s}$ ) [37].

After photosensitized oxidation of 10  $\mu\text{M}$  BSA by blue-light irradiation of 20  $\mu\text{M}$   $\text{Ru}(\text{bpy})_3^{2+}$ , the sample was diluted by 50 mM Na-phosphate pH 7 followed by 5 min adsorption of BSA at GCE, washing and SW voltammogram recording. After 5 min of photosensitization treatment, the YW peak of BSA decreased about by 40%, then slowly increased and levelled off after 45 min, when this peak achieved height by about 25% higher than that of native BSA (Fig. 2B). For longer irradiation times, slow decrease of YW peak was observed. The first fall of YW peak could be assigned to preferential oxidation of more solvent exposed residue Trp134, since time-resolved fluorescence spectra of BSA during mild photosensitization with  $\text{Ru}(\text{bpy})_3^{2+}$  demonstrated that Trp134 is quantitatively consumed by  $^1\text{O}_2$  to form side-chain formyl kynurenine as oxidation product, while the buried residue Trp213 was much less oxidized [36]. Subsequent increment of YW peak of BSA could be explained by subtle changes in the protein adsorption and/or by small conformational changes of oxidized BSA, accompanied by larger exposition of Tyr residues. In this context, we can suggest that the slower decrease of YW peak height after 45 min of photo-oxidation could be due to less efficient photo-oxidation of Tyr residues and/or of the hydrophobic Trp213 residue. In fact,  $^1\text{O}_2$ -reactivity at Trp was about 6-times stronger than that of Tyr, both in monomeric aa [29] and in BSA backbone [36], as detected by spectroscopy. In addition, it has been shown that diffusion of ground-state oxygen  $^3\text{O}_2$  (and also  $^1\text{O}_2$ ) into the Sudlow's site II, where the Trp213 is located [38], is about one-order of magnitude lower than in buffer precluding the oxidation of this inner residue [31,39]. Therefore, also positioning of the given residues in the BSA molecule influences its reactivity with  $^1\text{O}_2$ . Nevertheless, the evolution of the intensity of the SWV oxidation peak suggests that subtle structural changes were obtained between 5 and 45 min of photo-oxidation treatment. At

longer time, structural changes detection is difficult to assert, because oxidative damage of Tyr and Trp residues prevailed over the structural changes.

Moreover, the YW peak of photo-oxidized native BSA after 60 min was about four times smaller than YW peak of non-oxidized urea-denatured BSA, suggesting that  $^1\text{O}_2$ -mediated oxidation did not produce noticeable modification of the BSA structure, such as unfolding or denaturation [40]. Electrophoretic analysis by polyacrylamide gels (PAGE) of 100  $\mu\text{M}$  BSA done under native (not shown) and denaturing conditions [36], did not show any evidence of significant protein fragmentation, cross-linking or oligomerization.

Changes of YW peak were in agreement with changes of Trp residues obtained by spectroscopic methods (Table 1). Fluorescence intensity of Trp exponentially decreased while much smaller changes were observed in YW peak during photo-oxidation. Various responses could be explained by different principles of the applied methods. Steady-state and time-resolved spectroscopic data inform principally about changes of individual Trp residues in BSA, while our electrochemical data provide information about oxidizability of Trp and Tyr residues in the surface-attached BSA.

### 3.2. Detection of $^1\text{O}_2$ -induced protein damage at mercury electrode

#### 3.2.1. Bovine serum albumin

Recently, we showed that native BSA does not show any sign of denaturation close to the potential of zero charge but is denatured at the electrode surface due to prolonged exposure to negative potentials [20]. In CPS, the rate of potential changes increases with negative stripping current ( $I_{\text{str}}$ ) intensity, and at sufficiently negative  $I_{\text{str}}$  intensities the time of the protein exposure to negative potentials can be reduced to milliseconds. In such very short time intervals, the electric field-induced damage of the surface-attached protein can be negligible. Previously, we showed that the dependence of the protein peak H (due to catalytic hydrogen evolution reaction, CHER) on  $I_{\text{str}}$  displays the transition between native and denatured forms of protein [20,41]. Firstly, we compared the dependence of CPS peak H of non-oxidized native and urea-denatured BSA [42] on the  $I_{\text{str}}$  (at 26 °C). Between  $I_{\text{str}}$ –70 and –55  $\mu\text{A}$ , peak H heights of denatured BSA decreased with increasing negative  $I_{\text{str}}$  intensities, while peak heights of non-oxidized native BSA were close to zero (Fig. 3A). In this  $I_{\text{str}}$  region, very large differences between the CPS peaks of denatured and

native BSA were obtained. At less negative  $I_{\text{str}}$  intensities than –40  $\mu\text{A}$ , the peaks of native BSA and denatured BSA were almost identical, indicating denaturation of native BSA under the relatively slow electrode polarization. Between  $I_{\text{str}}$ –40 and –55  $\mu\text{A}$ , peak H heights of native BSA decreased with increasing negative  $I_{\text{str}}$  intensity much more steeply than those of denatured BSA (Fig. 3A) resembling curves indicating a structural transition. Electric field-driven transition is influenced also by factors, such as temperature, current intensity and particularly by the time of surface-attached protein exposure to the negative potentials [41]. Presence of 600 nM  $\text{Ru}(\text{bpy})_3^{2+}$  shifted structural transition between native and denatured BSA by about 20  $\mu\text{A}$  to more negative  $I_{\text{str}}$  value (not shown). A small peak of native BSA can be explained by low accessibility of catalytically active aa residues (Lys, Arg, His and Cys) [43,44], which are either buried inside the protein molecule and/or located to far from the electrode surface. These data are in good agreement with previous results obtained with BSA and other proteins [20,41,45].

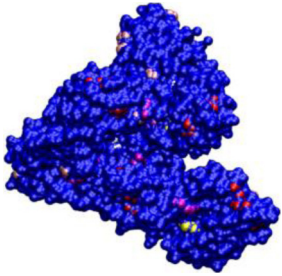
We compared CPS responses between native and photo-oxidized BSA by following the half  $I_{\text{str}}$  values ( $I_{\text{str}1/2}$ , Fig. 3A Inset) corresponding to the midpoint of the transition. Fig. 3B shows that during the first 15 min of BSA photo-oxidation the  $I_{\text{str}1/2}$  value almost did not change. However, with further photo-oxidation,  $I_{\text{str}1/2}$  shifted to more negative intensities and structural transition was broader than at shorter photo-oxidation times. On the other hand, no changes were observed in native BSA solutions in the presence of the sensitizer under dark conditions (Fig. 3B). The results suggest that presence of  $^1\text{O}_2$  makes the BSA less stable as compared to its non-oxidized native form. Electric field-induced denaturation, caused by exposure of the surface-attached protein to the negative potentials, appears in photo-oxidized BSA at shorter time of the potential exposure than in native BSA. Similar results we observed with another protein—urease from jack bean (Fig. 4).

#### 3.2.2. Urease

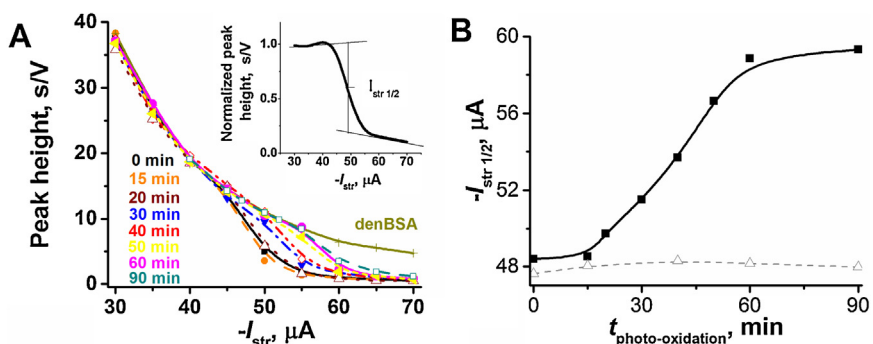
Using urease we were able to follow  $^1\text{O}_2$ -induced changes in the protein, both electrochemically and also with enzymatic activity measurements. Urease, hexameric enzyme with six active sites, catalyzes the breakdown of urea into ammonia and carbamate [46,47]. Electrochemical behavior and enzymatic activity of urease adsorbed at Hg-containing surfaces were earlier studied [20,26]. Here, we irradiated with blue light 50  $\mu\text{M}$  urease solutions in the

**Table 1**

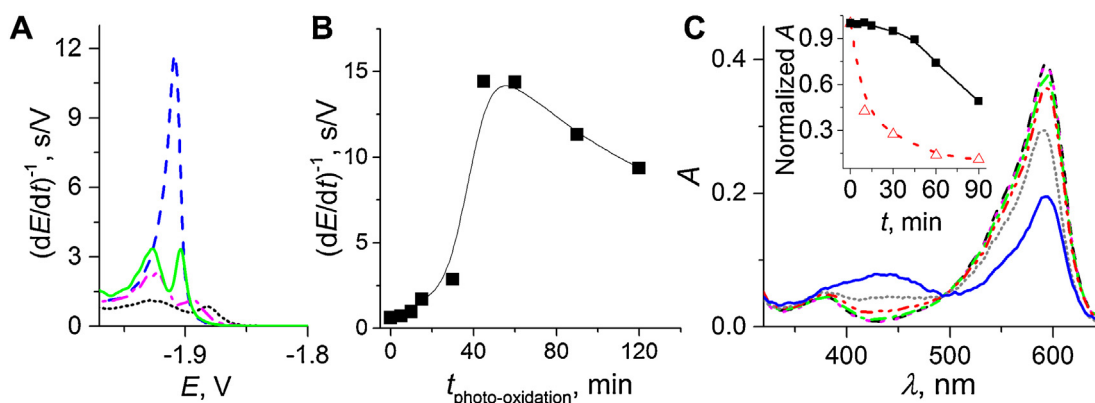
Changes in BSA properties after photo-oxidation (For interpretation of the references to color in the footnote, the reader is referred to the web version of this article.).

Method	Electro-active residues affected by $^1\text{O}_2$	Bovine serum albumin				ref.	structure/exposed surface
		Changes in BSA structure	Changes after photo-oxidation	Analysis performed			
SWV at carbon electrode	Tyr, Trp	local changes in 3D structure	5 min	at slightly positively charged surface	Fig. 2		
Emission fluorescence spectroscopy	Tyr, Trp	local changes in 3D structure	5 min	in solution	[36]		
CPS at mercury electrode	Cys, His	global changes in 3D structure	20 min	at negatively charged surface	Fig. 3		
SDS PAGE		no changes (fragmentation, oligomerization)	–	in the gel	[36]		

<sup>\*</sup> 3D view of BSA monomer (3V03) surface residues target of  $^1\text{O}_2$  colored (Tyr: magenta; His: pink; Trp: white; Met: yellow and Cys: red).



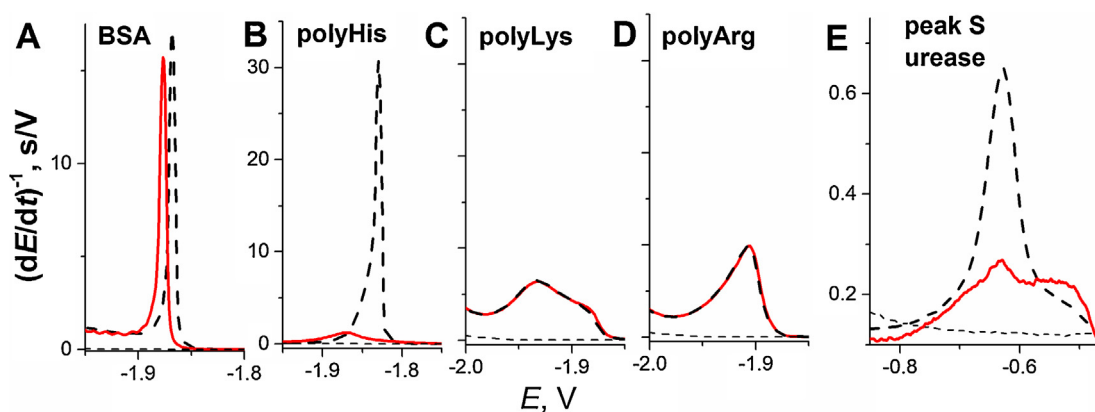
**Fig. 3.** A Dependence of *in situ* peak H height of native (0 min, —■—), 15 min (orange, —●—), 20 min (dark brown, —▲—), 30 min (blue, —▼—), 40 min (—◇—), 50 min (yellow, —◀—), 60 min (magenta, —●—), 90 min (cyan, —□—) photo-oxidized and urea-denatured (brown, —+—) BSA on stripping current,  $I_{str}$ . 300 nM BSA in presence of 600 nM  $Ru(bpy)_3^{2+}$  was adsorbed at accumulation potential,  $E_A$  0.1 V for accumulation time,  $t_A$  60 s from 50 mM Na-phosphate, pH 7 at HMDE followed by chronopotentiogram recording. Inset: Graphical representation of  $I_{str1/2}$  measurement. Peak height of photo-oxidized BSA is normalized to peak height of denatured BSA. B. Dependence of  $I_{str1/2}$  on time of BSA treatment with (—■—) and without photo-oxidation (—▲—). (For interpretation of the references to color in this figure legend, the reader is referred to the web version of this article.)



**Fig. 4.** A Peak H of urease at 0 min (black, ·····), 15 min (magenta, - - -), 30 min (green, —) and 90 min (blue, - - -) of photo-oxidation. B. Dependence of peak H height on time of photolysis. A., B. In *ex situ* experiments, 1  $\mu$ M urease was adsorbed at HMDE at open current potential for 2 min, followed by washing and transferring of the urease-modified HMDE to background electrolyte. Chronopotentiogram was recorded with  $I_{str}$  35  $\mu$ A. C. Absorption spectra of bromocresol corresponding to urease enzymatic activity in solution at 0 min (black, ·····), 15 min (magenta, - - -), 30 min (green, - - -), 45 min (red, - - -), 60 min (gray, ·····) and 90 min (blue, —) of photolysis. Inset: Dependence of absorbance at 592 nm correlated with enzymatic activity changes of urease in solution (black) and adsorbed at surface (red) on time of photo-oxidation treatment. (For interpretation of the references to color in this figure legend, the reader is referred to the web version of this article.)

presence of 100  $\mu$ M  $Ru(bpy)_3^{2+}$  to photo-oxidize the protein (Fig. 4). Urease peak H increased gradually during the first 35 min of the blue light treatment. In the next 10 min, this peak steeply rose (Fig. 4A, B) suggesting that the  $^1O_2$ -induced protein damage reached the level at which the surface-attached urease was

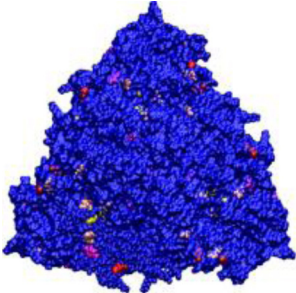
unfolded due to electric field effects at the negatively charged electrode surface [41,45]. This unfolding contrasted with small changes in peak H during the first 20 min of photo-oxidation, suggesting resistance of the photo-oxidized surface-attached urease to the electric field effects. After longer photo-oxidation



**Fig. 5.** *In situ* peak H of A. 300 nM BSA, 5  $\mu$ g/mL B. polyHis C. polyLys D. polyArg and E. *ex situ* peak S of 2  $\mu$ M urease after 0 min (black, - - -) and 60 min (red, —) of photo-oxidation in background electrolyte (black, ·····);  $I_{str}$  A. -40  $\mu$ A, B.-D.-22  $\mu$ A, E.-1  $\mu$ A. (For interpretation of the references to color in this figure legend, the reader is referred to the web version of this article.)

**Table 2**

Changes in urease properties after photo-oxidation (For interpretation of the references to color in the footnote, the reader is referred to the web version of this article.).

Method	Electro-active residues affected by $^1\text{O}_2$	Urease		Analysis performed	ref.	structure/exposed surface
		Changes in urease structure	Changes after photo-oxidation			
CPS at mercury electrode	Cys, His	global changes in 3D structure	40 min	at negatively charged surface	Fig. 4	
Enzyme activity	His, Cys His, Cys	decrease of activity decrease of activity	60 min 10 min	in solution at amalgam rod	Fig. 4 Fig. 4 Inset	

<sup>a</sup> 3D view of urease trimer (3LA4) surface residues target of  $^1\text{O}_2$  colored (Tyr: magenta; His: pink; Trp: white; Met: yellow and Cys: red).

time, protein oxidation accompanied by increased protein surface hydrophobicity could contribute to the protein unfolding [27]. Prolonged exposure to the negative potential during chronopotentiogram recording may enhance unfolding of destabilized protein attached at the surface. At photo-oxidation times longer than 60 min, urease peak H decreased and shifted to more negative potentials, probably because the damage of the electroactive residues prevailed over the structural changes. Also 60 min photo-oxidized BSA resulted in peak H decrease by about 10% and shift by about 20 mV to more negative potentials (whereby experimental error did not exceed 5%, Fig. 5A). This decrease and shift could result from  $^1\text{O}_2$ -mediated damage to electrocatalytically active aa residues [3,27] preventing thus their contribution to CHER. We tested influence of  $^1\text{O}_2$  on peak H of homo polyamino acids of His, Lys and Arg, involved in CHER. Peaks H of polyArg (Fig. 5C) and polyLys (Fig. 5D) were not affected after 60 min of photo-oxidation, while peak H of polyHis almost completely disappeared under the given experimental conditions (Fig. 5B). We tested influence of  $^1\text{O}_2$  treatment on Cys residues, which are also involved in CHER and react with  $^1\text{O}_2$ , using peak S at  $\sim -0.63$  V (due to reduction of Hg-S bonds, Fig. 5E). In contrast to peaks H, peaks S of BSA and urease were rather small and not well developed even at lower negative  $I_{\text{str}}$  intensity. However, urease peak S almost completely disappeared after 60 min photo-oxidation. These results agree with preferential His and Cys reactivity towards  $^1\text{O}_2$ .

### 3.3. Enzymatic activity of urease damaged by $^1\text{O}_2$

In contrast to changes of urease peak H, urease enzymatic activity measured in solution did not change up to 45 min (Fig. 4C, Table 2), while enzymatic activity of urease adsorbed at an amalgam rod decreased already after 10 min of photo-oxidation treatment (Fig. 4C Inset). This decrease of urease enzymatic activity can be explained by changes in enzyme active center, due to  $^1\text{O}_2$ -mediated oxidation of His and/or Cys residues [3,27]. The enzymatic center of urease, localized in a cavity, consists of two centers, where Ni ions are bound to 4 His, 1 Lys and 1 Asp residues [46,48]. A mobile flap, with a catalytically essential His, modulates the entrance of the substrate to the active site cavity [46,47]. The other critical residue located on this flap is Cys592, whose modification leads to impairing of the enzymatic activity [43].

We can expect that  $^1\text{O}_2$  generated in the bulk buffer diffused randomly into the solution and probably started to oxidize aa residues exposed at the urease surface. The short urease oxidation by  $^1\text{O}_2$  need not to change urease enzymatic center but may strongly influence urease adsorption at the metal surface and contribute to changes of urease electrocatalytic and activity responses. Earlier decrease in enzymatic activity of urease adsorbed at amalgam rod than of that in solution could be a result of conformational changes in the adsorbed protein either with significant changes at the secondary structural level or in the active site of the enzyme alone. Similar findings were obtained with urease modified by silver nanoparticles forming protein corona. The circular dichroism results clearly showed that formation of the protein corona induced drastic conformational changes in urease, leading to complete loss of the enzymatic activity [49]. We can speculate that after longer photo-oxidation treatment of urease,  $^1\text{O}_2$  oxidizes also aa residues hidden inside the molecule structure, what can be accompanied by decrease of enzymatic urease activity even in the solution.

The present data are in a good agreement with the results showing that the targets for  $^1\text{O}_2$  are predominantly tryptophan, tyrosine, histidine and cysteine residues in proteins [3,27] providing information about changes of BSA and urease induced by  $^1\text{O}_2$ .

## 4. Conclusion

Protein oxidation by reactive oxygen species belongs to irreversible posttranslational modifications, which ultimately lead to cell dysfunction and death [2] and play a key role in the development of various diseases [1]. Oxidation of proteins can induce a wide range of protein changes such as dimerization, aggregation, unfolding, conformational changes, etc. [1,3,27].

Electrochemical analyses utilizing intrinsic electroactivity of aa's, by means of CPS at Hg electrodes and/or by SWV at carbon electrodes, appeared as sensitive detection methods of changes in protein structure [13]. In this paper, we used these methods to study changes in proteins induced by  $^1\text{O}_2$  in complement to previous spectroscopic data [36]. We observed only relatively small changes in YW peak of photo-oxidized BSA as compared to those resulting from BSA unfolding and/or denaturation [11]. In

contrast, large changes in electrochemical responses of non- and photo-oxidized surface-attached BSA were obtained by CPS analysis as a result of tendency to destabilize oxidized BSA causing unfolding due to electric field effects at highly negative potentials [41,45]. Similar changes in CPS responses as those with BSA, were obtained for the photo-oxidation of urease. Changes in peak H appeared earlier than impairment in enzymatic activity in solution which required much longer photo-oxidation (Table 2). Our voltammetric results and data of enzymatic activity suggest that  $^1\text{O}_2$ -mediated changes did not induce unfolding of urease molecule in solution. On the other hand measurement of the enzymatic activity at metal surface and CPS analysis showed better sensitivity in detection of subtle changes in oxidatively damaged proteins probably due to local changes in protein structure after its adsorption at the surface, which enhanced unfolding of the destabilized protein. CPS analysis at HMDE was used for the first time to study of oxidative protein damage. HMDE provides better sensitivity and reproducibility than solid electrodes but it cannot compete with them in practical applications. Earlier we showed that solid amalgam electrodes yielded qualitatively similar results as those obtained with HMDE [13,22,41] but appeared convenient for parallel analysis [50].

Our methods utilizing intrinsic electrochemical signals of proteins could provide helpful information for better understanding of biological processes. We believe that this paper together with previous data obtained with proteins [13], such as p53 [16] and AGR2 showed interesting properties of surface-attached proteins and offered simple and inexpensive tools for protein research important in present proteomics and biomedicine.

## Acknowledgments

The authors are indebted to Dr. K. Réblová, Dr. V. Rey and Dr. I. Abatedaga for technical assistance. This research was supported by the bi-national cooperation program ARC/11/15 of MINCYT (Argentina)-MEYS (7AMB12AR028, Czech Republic) and by the Czech Science Foundation project No.13-00956S (to VO), and Argentinean research grants to CDB PIP-12-0374 (CONICET) and PICT-12-2666 (MINCYT).

## References

- [1] N. Chondrogianni, I. Petropoulos, S. Grimm, K. Georgila, B. Catalgol, B. Friguat, T. Grune, E.S. Gonos, Protein damage, repair and proteolysis, *Molecular Aspects of Medicine* 35 (2014) 1–71.
- [2] A. Bachi, I. Dalle-Donne, A. Scaloni, Redox proteomics: Chemical principles, methodological approaches and biological/biomedical promises, *Chem. Rev.* 113 (2013) 596–698.
- [3] M.J. Davies, The oxidative environment and protein damage, *Biochim. Biophys. Acta: Proteins Proteomics* 1703 (2005) 93–109.
- [4] C.L. Hawkins, P.E. Morgan, M.J. Davies, Quantification of protein modification by oxidants, *Free Radical Biol. Med.* 46 (2009) 965–988.
- [5] C.L. Bian, H.Y. Xiong, X.H. Zhang, Y. Ye, H.S. Gu, S.F. Wang, Electrochemical detection of BSA damage induced by Fenton reagents in room temperature ionic liquid, *Sensors Actuators B: Chem.* 169 (2012) 368–373.
- [6] C.L. Bian, H.Y. Xiong, X.H. Zhang, W. Wen, S.F. Wang, An electrochemical biosensor for analysis of Fenton-mediated oxidative damage to BSA using poly-o-phenylenediamine as electroactive probe, *Biosensors Bioelectron.* 28 (2011) 216–220.
- [7] Y.M. Wang, H.Y. Xiong, X.H. Zhang, S.F. Wang, Electrochemical study of bovine serum albumin damage induced by Fenton reaction using tris (2,2'-bipyridyl) cobalt (III) perchlorate as the electroactive indicator, *Electrochim. Acta* 67 (2012) 147–151.
- [8] O. Hammerich, J. Ulstrup, *Bioinorganic electrochemistry*, Springer, Dordrecht, Netherlands, 2008.
- [9] J.R. Winkler, H.B. Gray, Electron flow through metalloproteins, *Chem. Rev.* 114 (2014) 3369–3380.
- [10] P. Lopes, H. Dyrnesly, N. Lorenzen, D. Otzen, E.E. Ferapontova, Electrochemical analysis of the fibrillation of Parkinson's disease [small alpha]-synuclein, *Analyst* 139 (2013) 749–756.
- [11] V. Ostatna, H. Cernocka, K. Kurzatowska, E. Palecek, Native and denatured forms of proteins can be discriminated at edge plane carbon electrodes, *Anal. Chim. Acta* 735 (2012) 31–36.
- [12] V. Ostatná, V. Vargová, R. Hrstka, M. Ďurech, B. Vojtěšek, E. Paleček, Effect of His6-tagging of anterior gradient 2 protein on its electro-oxidation, *Electrochim. Acta* 150 (2014) 218–222.
- [13] E. Paleček, J. Tkac, M. Bartosik, T. Bertok, V. Ostatna, J. Paleček, Electrochemistry of nonconjugated proteins and glycoproteins. Toward sensors for biomedicine and glycomics, *Chem. Rev.* 115 (2015) 2045–2108.
- [14] J.S. Daniels, N. Pourmand, Label-free impedance biosensors: Opportunities and challenges, *Electroanalysis* 19 (2007) 1239–1257.
- [15] C.D. Borsarelli, L.J. Falomir-Lockhart, V. Ostatna, J.A. Fauerbach, H.H. Hsiao, H. Urlaub, E. Paleček, E.A. Jares-Erijman, T.M. Jovin, Biophysical properties and cellular toxicity of covalent crosslinked oligomers of alpha-synuclein formed by photoinduced side-chain tyrosyl radicals, *Free Radical Biol. Med.* 53 (2012) 1004–1015.
- [16] E. Paleček, V. Ostatna, H. Cernocka, A.C. Joerger, A.R. Fersht, Electrocatalytic monitoring of metal binding and mutation-induced conformational changes in p53 at picomole level, *J. Am. Chem. Soc.* 133 (2011) 7190–7196.
- [17] E. Paleček, V. Ostatna, M. Masarik, C.W. Bertoncini, T.M. Jovin, Changes in interfacial properties of alpha-synuclein preceding its aggregation, *Analyst* 133 (2008) 76–84.
- [18] J. Vacek, M. Zatloukalova, M. Havlikova, J. Ulrichova, M. Kubala, Changes in the intrinsic electrocatalytic nature of  $\text{Na}^+/\text{K}^+$  ATPase reflect structural changes on ATP-binding: Electrochemical label-free approach, *Electrochemistry Communications* 27 (2013) 104–107.
- [19] V. Ostatna, F. Kuralay, L. Trnkova, E. Paleček, Constant current chronopotentiometry and voltammetry of native and denatured serum albumin at mercury and carbon electrodes, *Electroanalysis* 20 (2008) 1406–1413.
- [20] H. Cernocká, V. Ostatná, E. Paleček, Enzymatic activity and catalytic hydrogen evolution in reduced and oxidized urease at mercury surfaces, *Anal. Chim. Acta* 789 (2013) 41–46.
- [21] V. Ostatna, H. Cernocka, E. Paleček, Protein structure-sensitive electrocatalysis at DTT-modified electrodes, *J. Am. Chem. Soc.* 132 (2010) 9408–9413.
- [22] E. Paleček, H. Cernocka, V. Ostatna, L. Navratilova, M. Brazdova, Electrochemical sensing of tumor suppressor protein p53-deoxyribonucleic acid complex stability at an electrified interface, *Anal. Chim. Acta* 828 (2014) 1–8.
- [23] I.E. Kochevar, R.W. Redmond, Photosensitized production of singlet oxygen, Singlet Oxygen, UV-A, and Ozone 319 (2000) 20–28.
- [24] G.T. Wondrak, M.K. Jacobson, E.L. Jacobson, Endogenous UVA-photosensitizers: mediators of skin photodamage and novel targets for skin photoprotection, *Photochem. Photobiol. Sci.* 5 (2006) 215–237.
- [25] E. Paleček, V. Ostatna, Electroactivity of nonconjugated proteins and peptides. Towards electroanalysis of all proteins, *Electroanalysis* 19 (2007) 2383–2403.
- [26] K.S.V. Santhanam, N. Jespersen, A.J. Bard, Application of a novel thermistor mercury-electrode to study of changes of activity of an adsorbed enzyme on electrochemical reduction and oxidation, *J. Am. Chem. Soc.* 99 (1977) 274–276.
- [27] M.J. Davies, Singlet oxygen-mediated damage to proteins and its consequences, *Biochem. Biophys. Res. Commun.* 305 (2003) 761–770.
- [28] R.H. Bisby, C.G. Morgan, I. Hamblett, A.A. Gorman, Quenching of singlet oxygen by Trolox C, ascorbate, and amino acids: Effects of pH and temperature, *J. Phys. Chem. A* 103 (1999) 7454–7459.
- [29] A. Michaeli, J. Feitelson, Reactivity of singlet oxygen toward amino-acids and peptides, *Photochem. Photobiol.* 59 (1994) 284–289.
- [30] E. Alarcon, A. Maria Edwards, A. Aspee, F.E. Moran, C.D. Borsarelli, E.A. Lissi, D. Gonzalez-Nilo, H. Poblete, J.C. Scaiano, Photophysics and photochemistry of dyes bound to human serum albumin are determined by the dye localization, *Photochem. Photobiol. Sci.* 9 (2010) 93–102.
- [31] M.B. Espeche Turbay, V. Rey, N.M. Arganaraz, F.E. Moran Vieyra, A. Aspee, E.A. Lissi, C.D. Borsarelli, Effect of dye localization and self-interactions on the photosensitized generation of singlet oxygen by rose bengal bound to bovine serum albumin, *J. Photochem. Photobiol. B: Biol.* 141 (2014) 275–282.
- [32] V. Brabec, V. Mornstein, Electrochemical-behavior of proteins at graphite-electrodes. 2. Electrooxidation of amino-acids, *Biophys. Chem.* 12 (1980) 159–165.
- [33] C. Tanielian, C. Wolff, M. Esch, Singlet oxygen production in water: Aggregation and charge-transfer effects, *J. Phys. Chem.* 100 (1996) 6555–6560.
- [34] V. Brabec, V. Mornstein, Electrochemical-behavior of proteins at graphite-electrodes. 1. Electrooxidation of proteins as a new probe of protein-structure and reactions, *Biochim. Biophys. Acta* 625 (1980) 43–50.
- [35] X.H. Cai, G. Rivas, P.A.M. Farias, H. Shiraiishi, J. Wang, E. Paleček, Potentiometric stripping analysis of bioactive peptides at carbon electrodes down to subnanomolar concentrations, *Anal. Chim. Acta* 332 (1996) 49–57.
- [36] R.E. Gimenez, V. Vargova, V. Rey, B.M. Espeche Turbay, I. Abatedaga, F.E. Moran Vieyra, V.I. Paz Zanini, J. Mecchia Ortiz, N. Katz, V. Ostatna, C.D. Borsarelli, Singlet oxygen-mediated oxidation of bovine serum albumin photosensitized by the tris(2,2'-bipyridine) ruthenium(II) ion, *Free Radical Biol. Med.* (2015) (under revision).
- [37] K.A. Majorek, P.J. Porebski, A. Dayal, M.D. Zimmerman, K. Jablonska, A.J. Stewart, M. Chruszcz, W. Minor, Structural and immunologic characterization of bovine, horse, and rabbit serum albumins, *Mol. Immunol.* 52 (2012) 174–182.
- [38] T. Peters Jr., The albumin molecule: Its structure and chemical properties, in: T. Peters (Ed.), *All About Albumin*, Academic Press, San Diego, 1995, pp. 9–II.
- [39] E. Alarcon, A. Maria Edwards, A. Aspee, C.D. Borsarelli, E.A. Lissi, Photophysics and photochemistry of rose bengal bound to human serum albumin, *Photochem. Photobiol. Sci.* 8 (2009) 933–943.

- [40] N. Tayeh, T. Rungassamy, J.R. Albani, Fluorescence spectral resolution of tryptophan residues in bovine and human serum albumins, *J. Pharm. Biomed. Anal.* 50 (2009) 107–116.
- [41] H. Černocká, V. Ostatná, E. Paleček, Protein structural transition at negatively charged electrode surfaces. Effects of temperature and current density, *Electrochim. Acta* 174 (2015) 356–360.
- [42] V. Ostatna, B. Dogan, B. Uslu, S. Ozkan, E. Palecek, Native and denatured bovine serum albumin. D.c. polarography, stripping voltammetry and constant current chronopotentiometry, *J. Electroanal. Chem.* 593 (2006) 172–178.
- [43] V. Dorcak, V. Ostatna, E. Palecek, Electrochemical reduction and oxidation signals of angiotensin peptides. Role of individual amino acid residues, *Electrochemistry Communications* 31 (2013) 80–83.
- [44] V. Vargova, M. Zivanovic, V. Dorcak, E. Palecek, V. Ostatna, Catalysis of hydrogen evolution by polylysine, polyarginine and polyhistidine at mercury electrodes, *Electroanalysis* 25 (2013) 2130–2135.
- [45] E. Palecek, V. Ostatna, Potential-dependent surface denaturation of BSA in acid media, *Analyst* 134 (2009) 2076–2080.
- [46] A. Balasubramanian, K. Ponnuraj, Crystal structure of the first plant urease from jack bean: 83 years of journey from its first crystal to molecular structure, *J. Mol. Biol.* 400 (2010) 274–283.
- [47] A. Juskiewicz, A. Zaborska, A. Laptas, Z. Olech, A study of the inhibition of jack bean urease by garlic extract, *Food Chem* 85 (2004) 553–558.
- [48] C. Follmer, Insights into the role and structure of plant ureases, *Phytochemistry* 69 (2008) 18–28.
- [49] S. Ponnuel, B. Subramanian, K. Ponnuraj, Conformational Change Results in Loss of Enzymatic Activity of Jack Bean Urease on Its Interaction with Silver Nanoparticle, *Protein J.* 34 (2015) 329–337.
- [50] P. Juskova, V. Ostatna, E. Palecek, F. Foret, Fabrication and characterization of solid amalgam electrodes array for bioanalytical applications, *Anal. Chem.* 82 (2010) 2690–2695.